Cell Reports, Volume *42*

Supplemental information

PRMT5 mediates FoxO1 methylation and subcellular localization to regulate lipophagy in myogenic progenitors

Kun Ho Kim, Stephanie N. Oprescu, Madigan M. Snyder, Aran Kim, Zhihao Jia, Feng Yue, and Shihuan Kuang

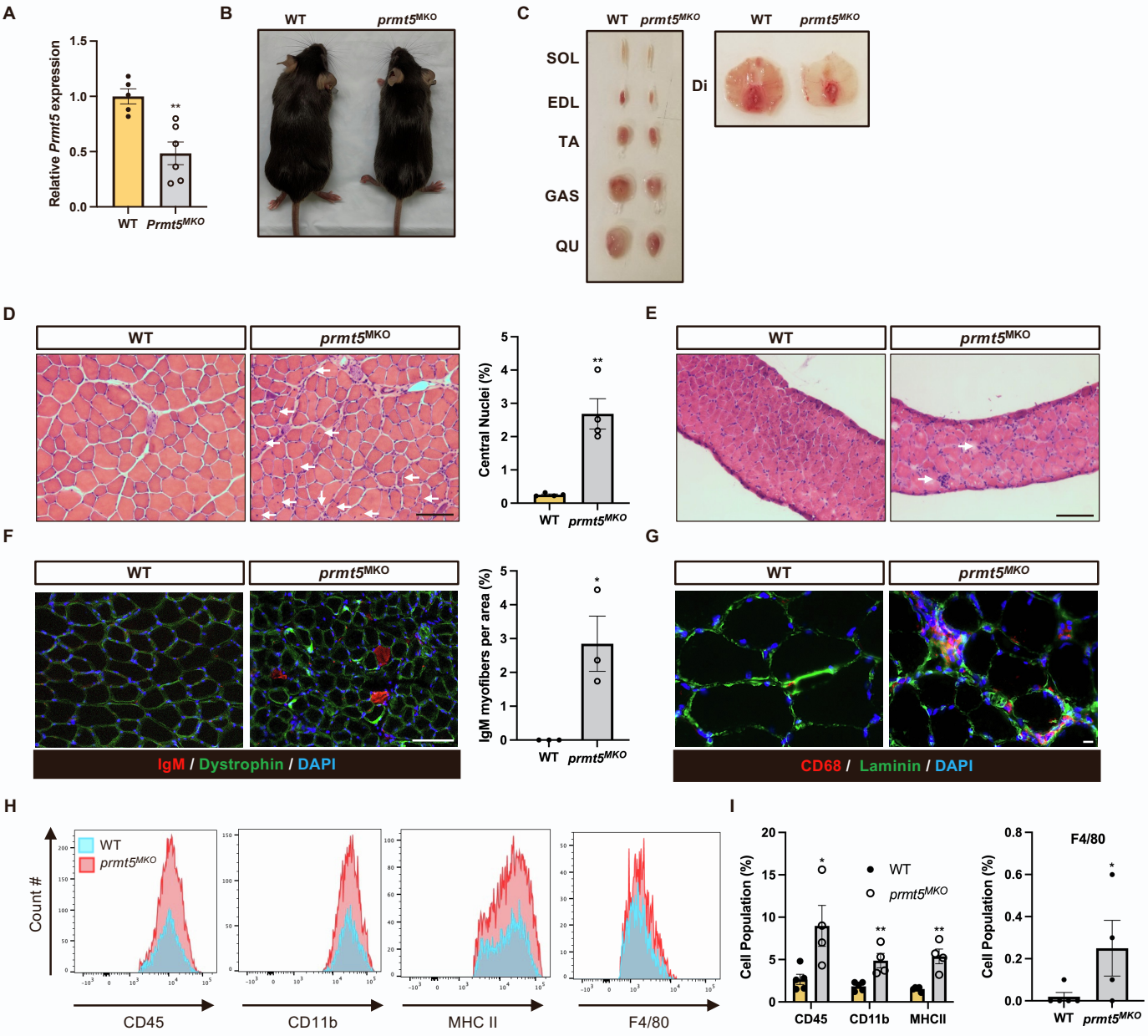

Figure S1: Loss of *Prmt5* in embryonic myoblasts leads to decrease in muscle mass and chronic inflammation in skeletal muscles, Related to Figure 1

(A) Decreased *Prmt5* mRNA expression in skeletal muscles isolated from *prmt5*^{MKO} mice compared to counterparts, n=5-6.

(B) Gross morphology of WT and *Prmt5*^{MKO} mice at 8 weeks of age.

(C) Gross morphology of muscle tissues including Sol, EDL, TA, GAS, QU, and Di in adult WT and *Prmt5*^{MKO} mice.

(D) H&E staining of WT and *prmt5*^{MKO} TA muscle sections (left panel) and quantification of centrally nucleated myofibers (right panel) (n=4), Arrowheads indicate central nuclei. Scale bar: 100 μm.

(E) H&E staining of WT and *Prmt5*^{MKO} Di muscle section, Arrowheads indicate nuclei clusters (Di). Scale bar: 100 μm.

(F) Immunofluorescence of IgM and Dystrophin (left panel) and corresponding quantification IgM^{+} myofibers (right panel) in TA muscle of WT and *Prmt5*^{MKO} mice. Scale Bar: 100 μm.

(G) Immunofluorescence of CD68 and Laminin in TA muscle of WT and *Prmt5*^{MKO} mice. Scale Bar: 10 μm.

(H and I) Flow cytometry analysis showing the histogram of immune cell population identified as CD45^{+}, CD11b^{+}, MHC II^{+}, F4/80^{+} cells from hindlimb muscles of adult WT and *Prmt5*^{MKO} mice (n=4-5) (I), along with its corresponding quantification analysis.

Values are expressed as mean ± SEM. * P < 0.05, ** P < 0.01 by t-test.

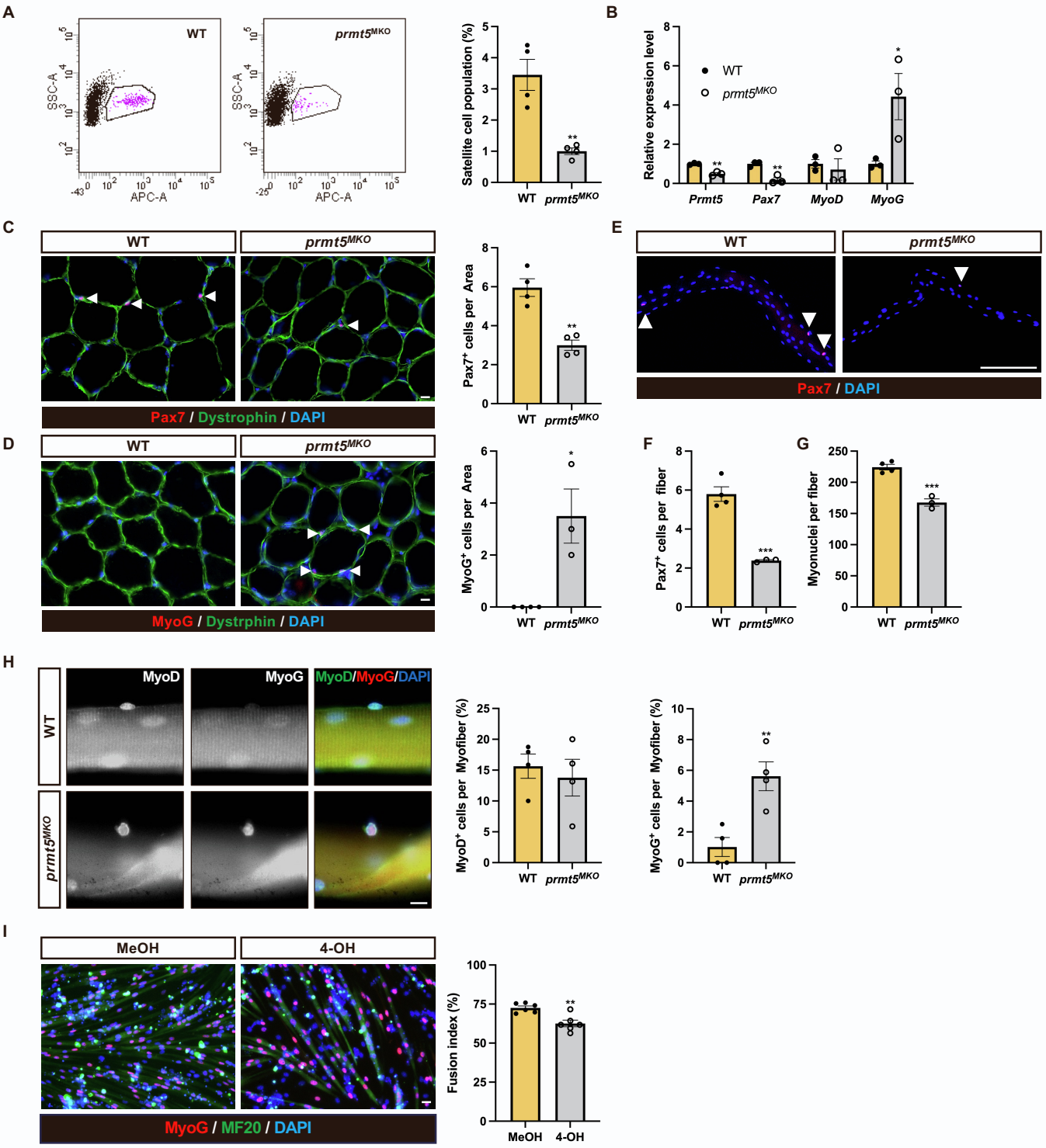

Figure S2: *Prmt5* knockout in embryonic myoblasts (*prmt5*^{MKO}) reduces number and increases MyoG$^+$ differentiating cell in adult mice, Related to Figure 3.

(A) Flow cytometry analysis showing distribution (left panel) and quantification (right panel) of satellite cells, identified as integrinα 7, (APC-A), lineage$^-$ (Sca1$^-$, CD31$^-$, CD45$^-$) cells freshly isolated from hindlimb muscles of adult WT and *Prmt5*^{MKO} mice (n=4).

(B) qPCR analysis of myogenic makers (*Pax7, Myod, Myog*) in skeletal muscles of adult WT and *Prmt5*^{MKO} mice (n=3).

(C and D) Immunofluorescence (left panel) and quantification (right panel) of Pax7$^+$ satellite cells (C) and MyoG$^+$ cells (D) per area in adult WT and *Prmt5*^{MKO} mice (n=4). Scale bar: 10 μm.

(E-G) Immunofluorescence of Pax7$^+$ cells (E) and quantification of Pax7$^+$ cells (F), and DAPI-marked myonuclei (G) per myofiber in freshly isolated EDL myofibers from adult WT and *Prmt5*^{MKO} mice (n=3). Scale bar: 100 μm.

(H) Immunofluorescence MyoD$^+$ and MyoG$^+$ cells (left panel) and quantification of MyoD$^+$ and MyoG$^+$ cells (right panel) per myofiber in freshly isolated EDL myofibers from adult WT and *Prmt5*^{MKO} mice (n=4). Scale bar: 10 μm.

(I) Immunofluorescence analysis of MyoG$^+$ cells and MF20$^+$ myotubes, followed by quantification of fusion index in 3-day differentiated control (MeOH) and *Prmt5* KO (4-OH) myotubes: 10 μm.

Values are expressed as mean ± SEM. * P < 0.05, ** P < 0.01, *** P < 0.001 by t-test

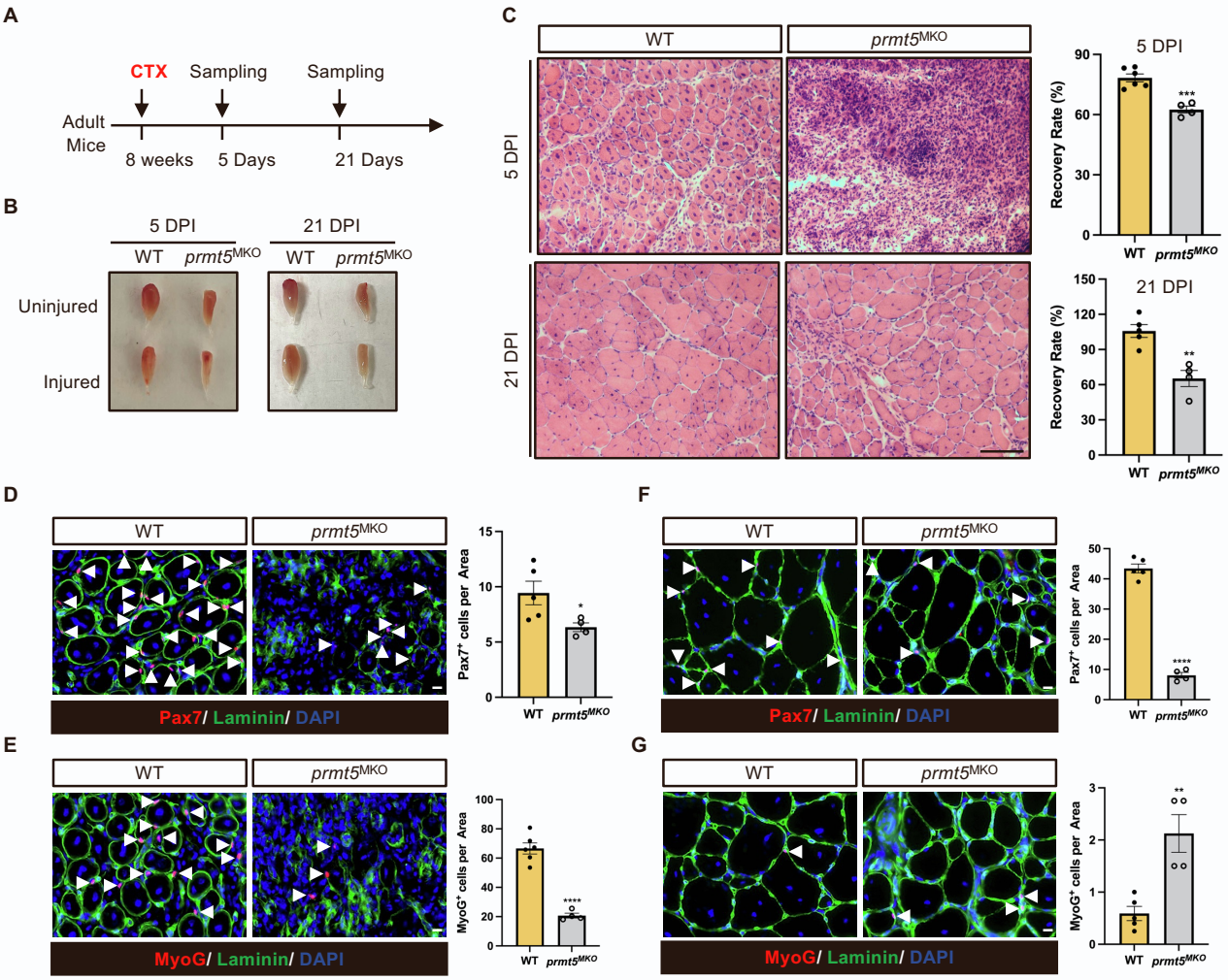

Figure S3: *Prmt5*^{MKO} mice exhibit impaired regenerative capacity upon muscle injury, Related to Figure 2.

(A) Experimental design to investigate muscle regeneration at day 5 and day 21 post CTX induced injury (DPI) in WT and *Prmt5*^{MKO} mice.

(B) Gross morphology of WT and *prmt5*^{MKO} TA muscles at 5- and 21-DPI.

(C) H&E staining of WT and *Prmt5*^{MKO} TA muscle sections (left panel) and recovery rate (right panel) at 5 and 21 DPI (n=4-5). Scale bar: 100 μm.

(D) Immunofluorescence of Pax7 and Laminin (left panel) and corresponding quantification of Pax7^{+} cells (right panel) of WT and *Prmt5*^{MKO} TA muscles at 5 DPI (n=4-5). Scale bar: 10 μm.

(E) Immunofluorescence of MyoG and Laminin (left panel) and corresponding quantification of MyoG^{+} cells (right panel) of WT and *Prmt5*^{MKO} TA muscles at 5 DPI (n=4-5). Scale bar: 10 μm.

(F) Immunofluorescence of Pax7 and Laminin (left panel) and corresponding quantification of Pax7^{+} cells (right panel) of WT and *Prmt5*^{MKO} TA muscles at 21 DPI (n=4-5). Scale bar: 10 μm.

(G) Immunofluorescence of MyoG and Laminin (left panel) and corresponding quantification of MyoG^{+} cells (right panel) of WT and *Prmt5*^{MKO} TA muscles at 21 DPI (n=4-5). Scale bar: 10 μm.

Values are expressed as mean ± SEM. * P < 0.05, ** P < 0.01, *** P < 0.001, **** P < 0.0001 by t-test.

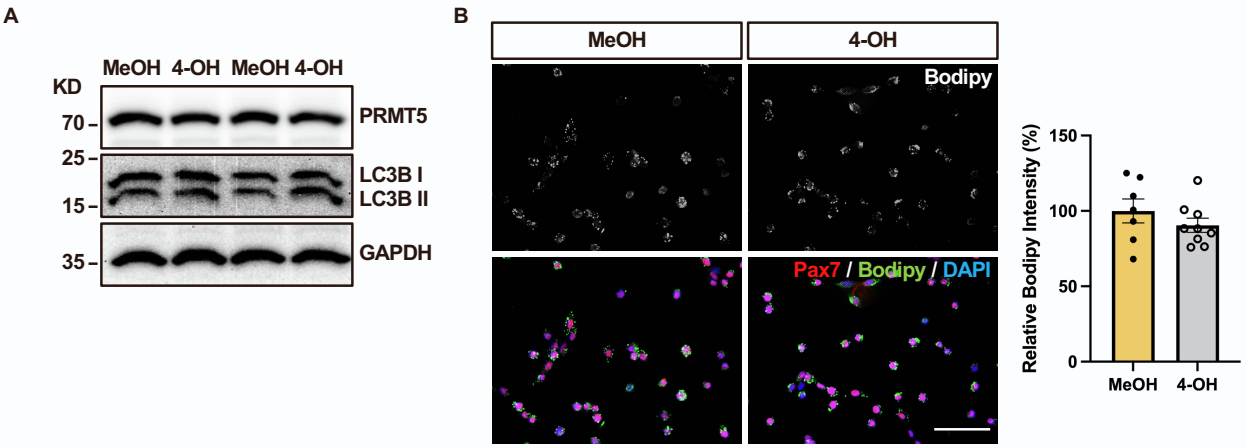

Figure S4: Tamoxifen (4-OH) does not affect the autophagy and lipid intensity in primary myoblasts, Related to Figure 4

(A) Western blotting showing the level of PRMT5 and LC3B, and GAPDH in the presence or absence of 4-OH in primary myoblast isolated from *Rosa*^{CreER}/*Prmt5*$^{flox/+}$ mice. KD: kilodalton band size marker.

(B) Pax7 and Bodipy immunofluorescence (left panel) and quantification of Bodipy intensity (right panel) in in primary myoblast isolated from *Rosa*^{CreER}/*Prmt5*$^{flox/+}$ mice in the presence or absence of 4-OH: 100 µm.

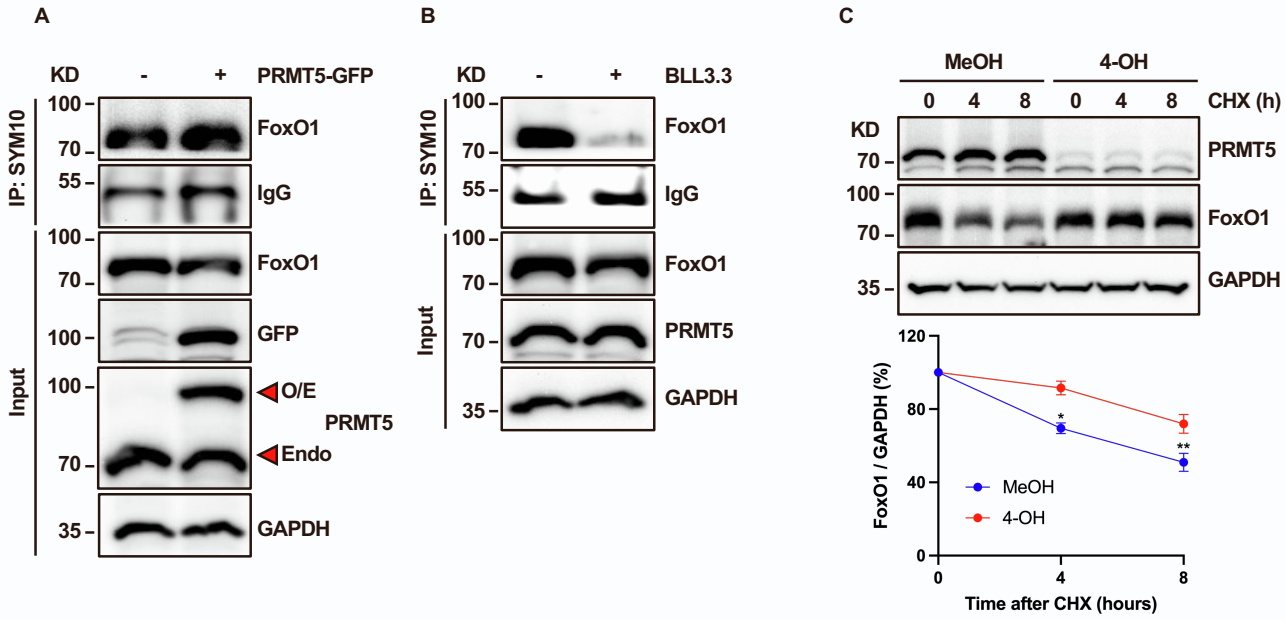

Figure S5: PRMT5 overexpression and inhibition mediates FoxO1 methylation in C2C12 myoblasts, Related to Figure 5

(A) C2C12 cells overexpressing PRMT5-GFP were immunoprecipitated with SYM10 antibody, and blotted with FoxO1, GFP, PRMT5, GAPDH

(B) C2C12 cells were immunoprecipitated with SYM10 antibody in the absence or presence of BLL3.3, PRMT5 inhibitor, and blotted with FoxO1, PRMT5, GAPDH

(C) Immunoblot analysis showing the FoxO1 protein levels in control (MeOH) and KO (4-OH) myoblasts, followed by treatment with cycloheximide (5 µg/ml) for 0,4, and 8 h. The intensity of FoxO1 was subsequently normalized to GAPDH, with 0 hours serving as the reference point (n=3, biological replicates). Values are expressed as mean ± SEM. * $P < 0.05$, ** $P < 0.01$ by t-test.

KD: kilodalton band size marker.

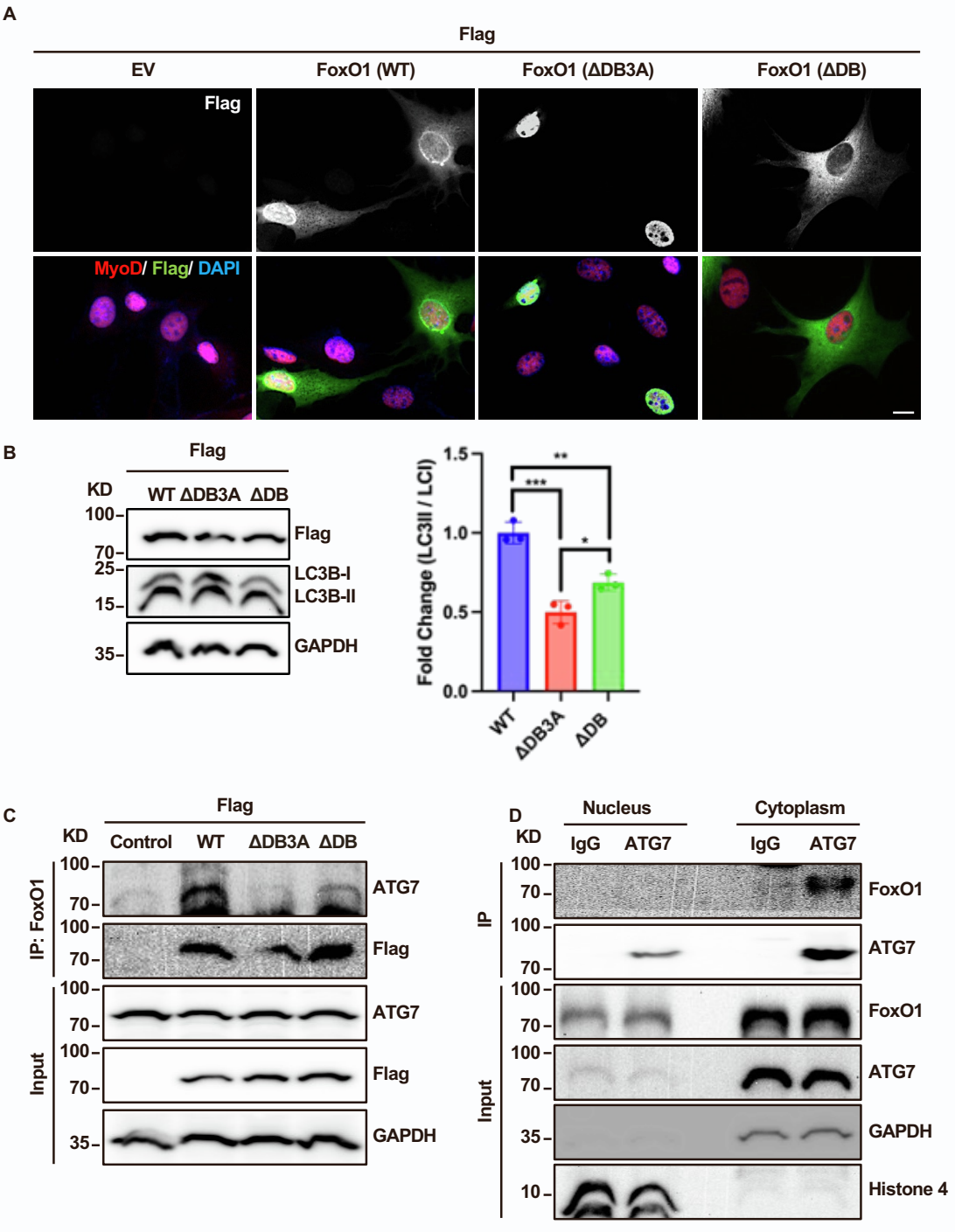

Figure S6: Cytoplasmic FoxO1 bins to ATG7 to induce autophagic activity in C2C12 myoblasts, Related to Figure 6

(A) Immunofluorescence analysis of MyoD, Flag, DAPI in C2C12 cells, following 24 hours of overexpression of Empty-Flag (EV), FoxO1-Flag (WT), ΔDB3A-Flag, and ΔDB-Flag. Scale bar: 10 um.

(B) Western blotting showing the levels of Flag, LC3B, and GAPDH in C2C12 cells subjected to a 24-hour overexpression of FoxO1-Flag (WT), ΔDB3A-Flag, and ΔDB-Flag (left panel), along with quantified levels (normalized to GAPDH) of LC3-II/I (right panel).

(C) C2C12 cells were subjected to a 24-hour overexpression of FoxO1-Flag (WT), ΔDB3A-Flag, and ΔDB-Flag. Whole cell lysates were immunoprecipitated with FoxO1 antibody and blotted with ATG7, Flag and GAPDH antibodies

(D) Primary myoblasts were immunoprecipitated with IgG or ATG7 antibody after subcellular fractionation and blotted with FoxO1, ATG7, GAPDH, and Histone 4 antibodies

Values are expressed as mean ± SEM. * $P < 0.05$, ** $P < 0.01$, *** $P < 0.001$ by t-test. KD: kilodalton band size marker.

Table S1. Primers used in this study. Related to STAR Methods

	Primer name		Sequence (5'->3')
qRT-PCR	*Prmt5*	Forward	CTGAATTGCGTCCCCGAAATA
		Reverse	AGGTTCCTGAATGAACTCCCT
	Pax7	Forward	CTGCTGAAGGACGGTCACTG
		Reverse	GGATGCCATCGATGCTGTGT
	MyoD	Forward	GGCTACGACACCGCCTACTA
		Reverse	CGACTCTGGTGGTGCATCTG
	MyoG	Forward	TGCCCAGTGAATGCAACTCC
		Reverse	TTGGGCATGGTTTCGTCTGG
	Pnpla2	Forward	GAGACCAAGTGGAACATC
		Reverse	GTAGATGTGAGTGGCGTT
	Lpl	Forward	GGGAGTTTGGCTCCAGAGTTT
		Reverse	TGTGTCTTCAGGGGTCCTTAG
	Fabp4	Forward	AAGGTGAAGAGCATCATAACCCT
		Reverse	TCACGCCTTTCATAACACATTCC
	Dgat1	Forward	TCCGTCCAGGGTGGTAGTG
		Reverse	TGAACAAAGAATCTTGCAGACGA
	Lc3B	Forward	ACAAAGAGTGGAAGATGTCCGGCT
		Reverse	TGCAAGCGCCGTCTGATTATCTTG
	Lamp1	Forward	TAGTGCCCACATTCAGCATCTCCA
		Reverse	TTCCACAGACCCAAACCTGTCACT
	Ulk1	Forward	AGATTGCTGACTTTGGATTC
		Reverse	AGCCATGTACATAGGAGAAC
	Beclin1	Forward	GGCCAATAAGATGGGTCTGA
		Reverse	GCTGCACACAGTCCAGAAAA
	Atg5	Forward	TAGAATATATCAGACCACGACG
		Reverse	CTCCTCTTCTCTCCATCTTC
	Atg7	Forward	GTGGGTCTTGTACTCACCACC
		Reverse	CCACTGAGGTTCACCATCCT
	Actin	Forward	GTCCCTCACCCTCCCAAAAG
		Reverse	GCTGCCTCAACACCTCAACCC